Astronomy & Astrophysics manuscript no. Miorita_vZLK
August 12, 2025

Letter to the Editor

Shepherding Miorita and its flock: A group of near-Earth asteroids driven by apsidal and von Zeipel-Lidov-Kozai secular resonances⋆

A source of low-perihelion asteroids

R. de la Fuente Marcos[1], C. de la Fuente Marcos[2], and O. Văduvescu[3]

[1] AEGORA Research Group, Facultad de Ciencias Matemáticas, Universidad Complutense de Madrid, Ciudad Universitaria, E-28040 Madrid, Spain
[2] Universidad Complutense de Madrid, Ciudad Universitaria, E-28040 Madrid, Spain
[3] University of Craiova, Str. A. I. Cuza 13, 200585, Craiova, Romania

Received 18 June 2025 / Accepted 28 July 2025

ABSTRACT

Context. Secular resonances can control the dynamical evolution of near-Earth asteroids (NEAs) and, in some cases, lead to increased orbital stability. Asteroid 622577 Miorita (2014 LU_{14}) was the first NEA found by the Isaac Newton Telescope (INT) and exhibits unusual dynamical traits although it approaches Venus, Earth, and Mars at relatively close range.
Aims. Here, we investigate the orbital context of Miorita and search for possible dynamical analogs within the NEA population.
Methods. We studied the orbital evolution of Miorita using direct N-body calculations. We used the NEOMOD 3 orbital distribution model to verify our conclusions. Observational data were obtained with INT's Wide Field Camera.
Results. Miorita is subjected to a von Zeipel-Lidov-Kozai secular resonance, but it is also in a near apsidal resonance, both controlled by Jupiter. We identified a group of dynamical analogs of Miorita that includes 387668 (2002 SZ), 2004 US_1, 299582 (2006 GQ_2), and 2018 AC_4. Miorita-like orbits can evolve into metastable, low-perihelion trajectories driven by apsidal and von Zeipel-Lidov-Kozai secular resonances like those of 504181 (2006 TC) and 482798 (2013 QK_{48}). Objects in such paths may end up drawn into the Sun.
Conclusions. Concurrent secular resonances tend to stabilize the orbits of these asteroids as they are protected against collision with Earth and other inner planets by the resonances. This group signals the existence of an active dynamical pathway capable of inserting NEAs in comet-like orbits. NEOMOD 3 gives a low probability for the existence of NEAs like Miorita, 504181 or 482798.

Key words. minor planets, asteroids: general – minor planets, asteroids: individual: 622577 Miorita (2014 LU_{14}) – methods: numerical – celestial mechanics

1. Introduction

Jupiter destabilizes the main asteroid belt, keeping dynamical pathways leading into Earth-crossing orbits open (see, e.g., Nesvorný et al. 2023, 2024a,b; Deienno et al. 2025). In this way, the near-Earth asteroid (NEA) population gathers new members that replace those lost to the Sun, to the inner planets, or ejected towards the outer regions of the Solar System. However, Jupiter's gravitational perturbation not only makes asteroid orbits unstable, in certain cases it may also turn unstable orbits into stable ones, decreasing the probability of planetary encounters and delaying/preventing eventual collisions (Milani et al. 1989).

Mean-motion resonances between asteroids and Jupiter produce the Kirkwood gaps in the main asteroid belt (see, e.g., Dermott & Murray 1983). In addition, secular resonances induced by Jupiter can sometimes make orbits unstable but, in other cases, these secular perturbations may lead to enhanced orbital stability (see, e.g., Froeschle et al. 1995; Vinogradova 2017, 2024). Increased local orbital stability causes the formation of dynamical groups.

Asteroid 622577 Miorita (2014 LU_{14}) was the first NEA found from La Palma by the Isaac Newton Telescope (INT, Tudor et al. 2014; Vaduvescu et al. 2015); its assigned name is an old Romanian pastoral ballad.[1] It exhibits unusual dynamical traits perhaps compatible with orbital stabilization via secular resonances. Here, we use N-body simulations to explore its dynamical context and implications. This Letter is organized as follows. In Sect. 2, we introduce the background of our work, and present the data and tools used in our analyses. In Sect. 3, we explore the orbital properties and resonant context of Miorita, and its probable origin together with those of a sample of dynamical analogs. In Sect. 4, we discuss our results and Sect. 5 summarizes our conclusions. Appendices include supporting material.

2. Context, methods, and data

In this section, we revisit dynamical concepts that are later used in our analysis. Software tools and data are also discussed here.

Send offprint requests to: R. de la Fuente Marcos, e-mail: rauldelafuentemarcos@ucm.es

⋆ Based on observations made with the Isaac Newton Telescope (INT), in the Spanish Observatorio del Roque de los Muchachos of the Instituto de Astrofísica de Canarias (IAC, program ID 136-INT9/14A).

[1] "Miorița is a unique Romanian pastoral myth-ballad. A little ewe with supernatural powers denounces the evil plan of two shepherds to murder her master. But this shepherd resigns himself to his fate, asking to be buried by the sheepfold and imagining his cosmic wedding witnessed by nature, Sun, Moon, torch stars and one falling star, meaning his death." Ref: WGSBN Bull. 4, #11, 22

2.1. Dynamics background

Secular resonances are organized into two different types, those affecting the precession of, e.g., the line of apsides and a resonant mechanism that exchanges eccentricity, e, and inclination, i, driving antiparallel oscillations or librations of these two orbital elements, the von Zeipel-Lidov-Kozai secular resonance (von Zeipel 1910; Kozai 1962; Lidov 1962; Naoz 2016; Sidorenko 2018; Ito & Ohtsuka 2019; Tremaine 2023). An apsidal resonance between an asteroid and a planet appears when there is a periodic libration of the relative apsidal longitude or relative longitude of perihelion, $\Delta\varpi = \varpi - \varpi_{\rm P}$ (see, e.g., Nakai & Kinoshita 1985; Scholl & Froeschle 1986), where $\varpi = \Omega + \omega$ is the longitude of perihelion of the asteroid, $\varpi_{\rm P} = \Omega_{\rm P} + \omega_{\rm P}$ is the one of the planet, Ω is the longitude of the ascending node of the asteroid and ω is its argument of perihelion, $\Omega_{\rm P}$ and $\omega_{\rm P}$ are the equivalent parameters for the planet (see, e.g., Murray & Dermott 1999). An extensive map of secular resonances in the NEA region was computed by Fenucci et al. (2023). Secular resonances play a prominent role on the dynamical evolution of extrasolar planetary systems (see, e.g., Zhou & Sun 2003; Libert & Tsiganis 2009; Lei & Gong 2022).

2.2. Data, data sources, and tools

Apollo-class NEA 622577 Miorita (2014 LU_{14}) was initially reported on June 2, 2014, by the EUROpean Near Earth Asteroids Research (EURONEAR, Vaduvescu et al. 2008)[2] project observing with the Isaac Newton Telescope (INT) from La Palma; it was announced on June 6 with the provisional designation 2014 LU_{14} (Tudor et al. 2014). The initial orbit solution was further improved using observations obtained by EURONEAR (see discussion in Appendix A) and other collaborations. Its orbital solution in Table A.1 is currently based on 95 observations with an observational timespan of 3644 d, and it is referred to epoch JD 2460800.5 TDB. It was retrieved from Jet Propulsion Laboratory's (JPL) Small-Body Database (SBDB)[3] provided by the Solar System Dynamics Group (SSDG, Giorgini 2011, 2015).[4] For Miorita, the Spitzer mission gives an absolute magnitude of 19.89±0.33 mag, a diameter of $0.357^{+0.142}_{-0.074}$ km, and an albedo of $0.151^{+0.100}_{-0.075}$ (Gustafsson et al. 2019). The object attracted our attention because it experiences relatively close encounters with Venus, the Earth–Moon system, and Mars.

The orbit of Miorita crosses those of Venus, the Earth–Moon system, and Mars. Periodic planetary close encounters might make the reconstruction of Miorita's past orbital evolution and the prediction of its future behavior beyond a few kyr difficult. In such cases, the orbital evolution has to be investigated statistically considering the uncertainties of the orbital solution. The calculations needed to study the evolution of Miorita were carried out using a direct N-body code described by Aarseth (2003) and publicly available from the web site of the Institute of Astronomy of the University of Cambridge.[5] This software implements the Hermite numerical integration scheme introduced by Makino (1991). Details and results from this code can be found in de la Fuente Marcos & de la Fuente Marcos (2012). Our physical model included the perturbations by the eight major planets, the Moon, the barycenter of the Pluto-Charon system, and the 19 largest asteroids, Ceres, Pallas, Vesta, Hygiea, Europhrosyne, Interamnia, Davida, Herculina, Eunomia, Juno, Psyche, Europa, Thisbe, Iris, Egeria, Diotima, Amphitrite, Sylvia, and Doris. For accurate initial positions and velocities (see Appendix B), we used data based on the DE440/441 planetary ephemeris (Park et al. 2021) from JPL's SSDG `Horizons` online Solar system data and ephemeris computation service.[6] Most input data were retrieved from SBDB and `Horizons` using tools provided by the `Python` package `Astroquery` (Ginsburg et al. 2019) and its `HorizonsClass` class.[7] Figures were produced using `Matplotlib` (Hunter 2007). The plausibility of our conclusions was examined within the context of the NEOMOD 3 orbital distribution model (Nesvorný et al. 2024b). NEOMOD 3 is the latest update of the NEOMOD project (Nesvorný et al. 2023, 2024a).

3. Results: Orbital evolution

Here, we use N-body simulations to assess the current dynamical status of 622577 Miorita (2014 LU_{14}) and its implications. Figure 1 shows the time evolution of the orbital elements of Miorita and summarizes the results of our calculations. The central panels focus on the short-term evolution of the nominal orbit and those of representative control orbits or clones with state vectors (Cartesian coordinates and velocities, see Table B.1 in Appendix B) well away from the nominal one, up to $\pm 9\sigma$ from the nominal orbital solution in Table A.1. Given the reasonable good quality of this orbital solution, even a deviation of $\pm 9\sigma$ in the values of the orbital elements gives a clone with initial conditions separated <0.001% from the nominal ones. The central panels of Fig. 1 show that control orbits that start arbitrarily close tend to diverge on a timescale of a few kyr, due to the effect of close encounters with Earth. In addition, the panels of e and i display anticorrelated librations of these two orbital elements with a period of 30,000 yr, signaling the presence of the von Zeipel-Lidov-Kozai secular resonance (von Zeipel 1910; Kozai 1962; Lidov 1962). All the control orbits studied (10^3) exhibit anticorrelated periodic libration of eccentricity and inclination.

To investigate the sources of orbital divergence (chaotic evolution) and von Zeipel-Lidov-Kozai oscillations, the nominal orbit was integrated using physical models that removed the Earth–Moon system or Jupiter; our results are shown on the left panels of Fig. 1. Looking at the evolution of the nominal orbit and the full physical model (in black), and that of the model with the Earth–Moon system removed (in blue), we observe that the kinks in the evolution of e and i dissapear, a confirmation that close planetary encounters are responsible for the onset of the observed chaotic behavior. In contrast, the removal of Jupiter (in brown) has a dramatic effect on the dynamical evolution of Miorita, the von Zeipel-Lidov-Kozai oscillations dissapear. In general, Jupiter fully controls the evolution of the shape (e) and the orientation in space (i, Ω, and ω) of the orbit of Miorita.

Figure 1, right panels, shows the results of longer integrations back into the past and forward into the future. These integrations delve deeper into the evolution displayed in the central panels. Although Miorita's orbital evolution is conspicuously chaotic, it is also clear that it remains confined to a relatively narrow volume of the orbital parameter space. One of the relevant control orbits, the one with state vectors separated -3σ from the nominal ones (in lime) deserves detailed study as it reaches a region in which additional secular resonances emerge. The long-term evolution of this control orbit is displayed in Figs. D.1 and

[2] http://www.euronear.org/
[3] https://ssd.jpl.nasa.gov/tools/sbdb_lookup.html#/
[4] https://ssd.jpl.nasa.gov/
[5] https://people.ast.cam.ac.uk/ sverre/web/pages/nbody.htm
[6] https://ssd.jpl.nasa.gov/horizons/
[7] https://astroquery.readthedocs.io/en/latest/jplhorizons/jplhorizons.html

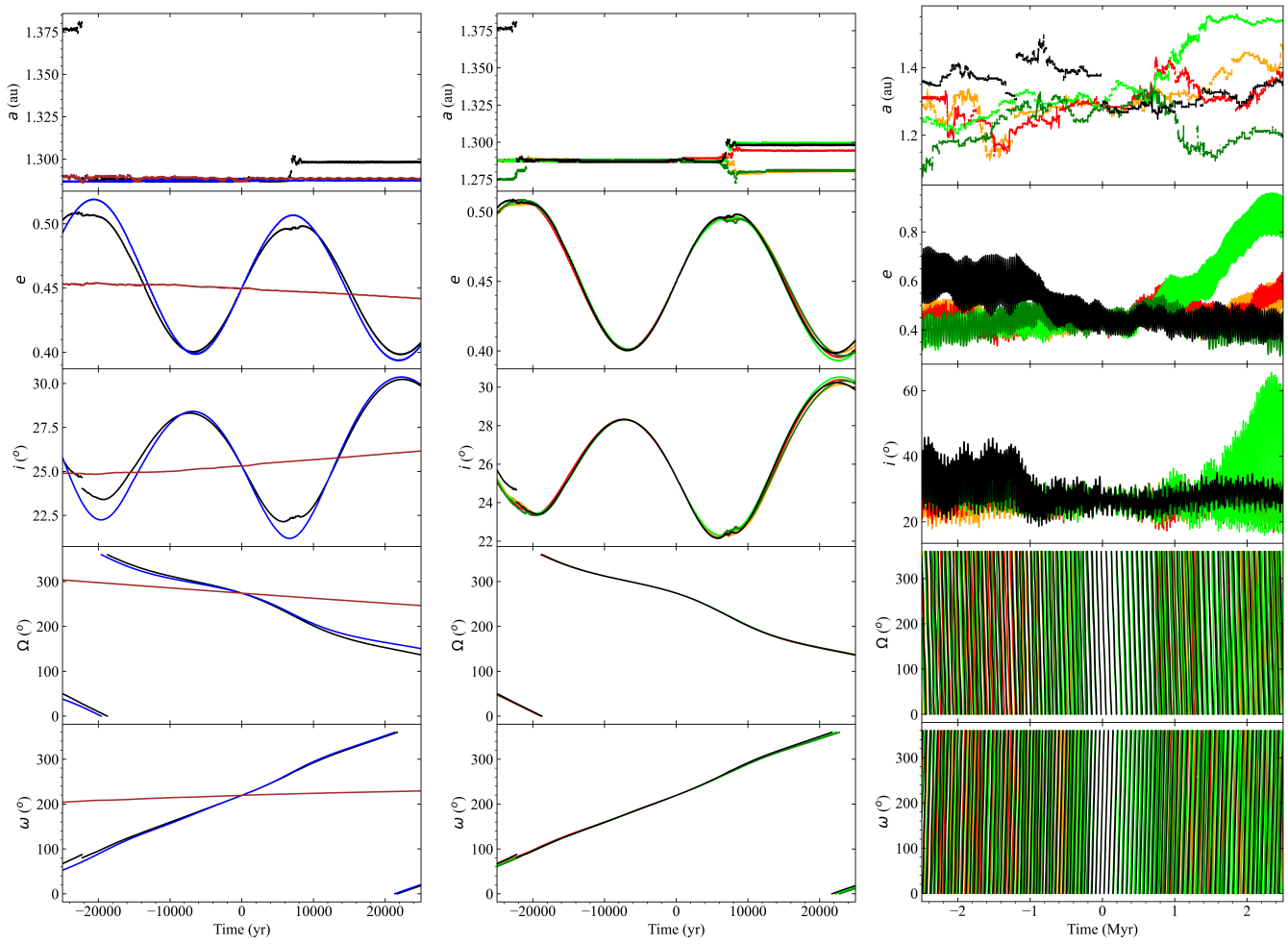

Fig. 1. Orbital evolution of 622577 Miorita (2014 LU_{14}). *Left panels:* Results of a simulation of the nominal orbit and the full physical model (in black), after removing the Earth–Moon system (in blue), and after removing Jupiter (in brown). *Central panels:* Short-term results of the full physical model and the nominal orbit (in black), those of control orbits with state vectors separated $\pm 3\sigma$ from the nominal ones in lime/green, and $\pm 9\sigma$ in orange/red. *Right panels:* Integrations in the central panels but on a longer timespan. Time evolution of the value of the semimajor axis, a (top panels), eccentricity, e (second to top), inclination, i (middle), the longitude of the ascending node, Ω (second to bottom), and the argument of perihelion, ω (bottom). The origin of time is the epoch 2460800.5 JD Barycentric Dynamical Time (2025-May-05.0 00:00:00.0 TDB) and the output cadence is 36.525 d for the left and central panels, and 25 yr for the right panels. The source of the input data is JPL's `Horizons`.

2. In addition to the short-period anticorrelated oscillations of e and i, a long-period (~2 Myr) oscillation emerges that is triggered by the onset of an apsidal resonance with Jupiter as shown in Fig. 2, top panel. The resonance is about $\varpi - \varpi_5 = 180°$ so the perihelia of Jupiter and Miorita are antialigned, when Miorita reaches perihelion, Jupiter is at aphelion and vice versa. From Figs. C.1 and C.2 of Appendix C, Miorita evolves close or inside this secular resonance.

4. Discussion

An important open question is how frequent Miorita-like orbits are. To estimate the theoretical likelihood of NEAs like 622577 Miorita (2014 LU_{14}), we considered the NEOMOD 3 orbital distribution model (Nesvorný et al. 2024b). This tool can be used to generate synthetic NEA populations suitable to estimate probabilites or test hypotheses, and reject or accept them; the model can only be strictly applied to objects with $H < 28$ mag and does not include fragmentations. We have generated a population of $2.75{\times}10^8$ synthetic NEOs of sizes above 0.001 km with the NEOMOD 3 simulator.[8] For our purposes, NEOMOD 3 generates a set of synthetic NEO instances characterized by a, e, i, and H. From this set, the probability (in the usual sense of number of occurrences in a sample of a certain size) of finding one object with values of its orbital elements (a, e, i) matching those of Miorita in Fig. 1, central panels — namely (1.275, 1.375) au, (0.39, 0.51), and (22, 30)°, respectively — is 0.0016.

Against this theoretical estimate, we can compare the one from real data. Querying JPL's SBDB within the volume of the orbital parameter space defined by the intervals above, we found 34 objects out of 38631 known NEAs, or a probability close to 0.0009, that is somewhat consistent with the one derived from NEOMOD 3 above, and indicative that such orbits are not long-term stable. Examples of dynamical analogs of Miorita are 387668 (2002 SZ), 2004 US_1, 299582 (2006 GQ_2), and 2018 AC_4 (see Fig. C.3 in Appendix C). But Miorita-like orbits may evolve into paths affected by an apsidal resonance with Jupiter.

Among NEAs with reliable orbits, we found two in paths similar to the one described in the previous section and affected

[8] https://www.boulder.swri.edu/~davidn/NEOMOD_Simulator/

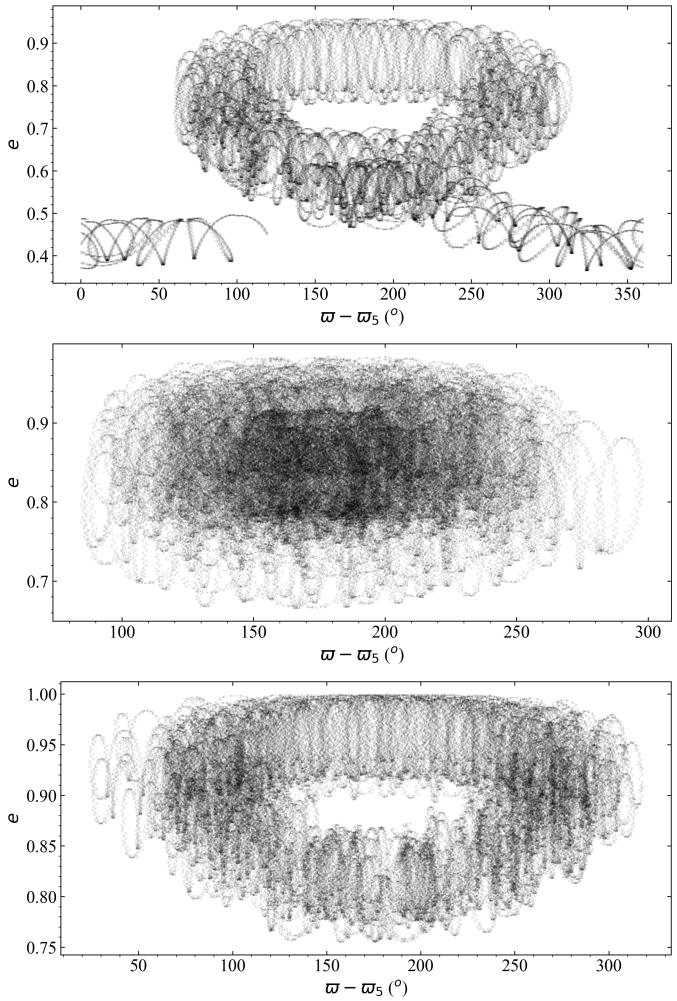

Fig. 2. Variation of the eccentricity with the relative (to Jupiter) apsidal longitude $\varpi - \varpi_5$. *Top panel:* Results for the control orbit of Miorita with state vectors separated -3σ from the nominal ones. *Middle panel:* Results for 504181 (2006 TC). *Bottom panel:* Results for 482798 (2013 QK_{48}). The source of the input data is JPL's `Horizons`.

by an apsidal resonance with Jupiter: 504181 (2006 TC) and 482798 (2013 QK_{48}), see Fig. 2. NEA 504181 evolves within the ranges of a, e and i, (1.48, 1.67) au, (0.60, 0.98), and (18, 70)°; for 482798, the equivalent intervals are (1.54, 1.70) au, (0.75, 1.0), and (10, 90)° (see Appendix D). Using NEOMOD 3, the probability of finding one NEA like 504181 is 0.0022, and for 482798 is 0.00057. Querying JPL's SBDB, we found for the case of 504181 100±10 (Poisson counting uncertainty) objects there, out of 38631 known NEAs, or a probability close to 0.0026; for 482798, the associated probability is 0.0009 (33±6 objects). The region inhabited by 504181 is nearly four times more stable than that of 482798. In fact, 482798-like orbits tend to be lost to the Sun (see Appendix D). The existence of such low-perihelion asteroids was predicted by Fenucci et al. (2023).

5. Summary and conclusions

In this Letter, we presented an investigation of the current dynamical status of Apollo-class NEA 622577 Miorita (2014 LU_{14}). Our conclusions can be summarized as follows.

1. We show that Miorita is concurrently engaged in a von Zeipel-Lidov-Kozai secular resonance and a near apsidal resonance, both driven by Jupiter. Concurrent secular resonances tend to stabilize the orbits of these asteroids.
2. We find that a number of NEAs move in Miorita-like orbits.
3. We find that objects in such orbits may become low-perihelion asteroids concurrently engaged into von Zeipel-Lidov-Kozai oscillations and an apsidal resonance, driven by Jupiter. Some known asteroids exhibit this behavior.

Our numerical study has confirmed the existence of an active dynamical pathway capable of inserting NEAs in comet-like orbits; this pathway was originally predicted by Fenucci et al. (2023). Such objects may pose as extinct-comet impostors.

Acknowledgements. We thank the anonymous referee for a constructive and timely report. RdlFM acknowledges funding from the "ENIMUS" Advanced Grant from the European Research Council (ERC) under the European Union's Horizon 2020 research and innovation programme (grant agreement ID 101097905). This work was partially supported by the Spanish 'Agencia Estatal de Investigación (Ministerio de Ciencia e Innovación)' under grant PID2020-116726RB-I00 /AEI/10.13039/501100011033. Based on observations made with the Isaac Newton Telescope (INT), installed at the Spanish Observatorio del Roque de los Muchachos of the Instituto de Astrofísica de Canarias, on the island of La Palma. In preparation of this Letter, we made use of the NASA Astrophysics Data System, the ASTRO-PH e-print server, and the Minor Planet Center (MPC) data server.

References

Aarseth, S. J. 2003, Gravitational N-Body Simulations (Cambridge: Cambridge University Press), 27
de la Fuente Marcos, C. & de la Fuente Marcos, R. 2012, MNRAS, 427, 728
Deienno, R., Denneau, L., Nesvorný, D., et al. 2025, Icarus, 425, 116316
Dermott, S. F. & Murray, C. D. 1983, Nature, 301, 201
Fenucci, M., Gronchi, G. F., & Novaković, B. 2023, A&A, 672, A39
Froeschle, C., Hahn, G., Gonczi, R., et al. 1995, Icarus, 117, 45
Ginsburg, A., Sipőcz, B. M., Brasseur, C. E., et al. 2019, AJ, 157, 98
Giorgini, J. 2011, in Journées Systèmes de Référence Spatio-temporels 2010, ed. N. Capitaine, 87–87
Giorgini, J. D. 2015, IAUGA, 22, 2256293
Gustafsson, A., Trilling, D. E., Mommert, M., et al. 2019, AJ, 158, 67
Hunter, J. D. 2007, Computing in Science and Engineering, 9, 90
Ito, T. & Ohtsuka, K. 2019, Monogr. Environ. Earth Planets, 7, 1
Kozai, Y. 1962, AJ, 67, 591
Lei, H. & Gong, Y.-X. 2022, A&A, 665, A62
Lidov, M. L. 1962, Planet. Space Sci., 9, 719
Libert, A.-S. & Tsiganis, K. 2009, A&A, 493, 677
Makino, J. 1991, ApJ, 369, 200
Masiero, J. R., Kwon, Y. G., Dahlen, D. W., et al. 2024, PSJ, 5, 113
Milani, A., Carpino, M., Hahn, G., et al. 1989, Icarus, 78, 212
Murray, C. D., & Dermott, S. F. 1999, Solar System Dynamics (Cambridge: Cambridge University Press)
Nakai, H. & Kinoshita, H. 1985, Celestial Mechanics, 36, 391
Naoz, S. 2016, ARA&A, 54, 441
Nesvorný, D., Deienno, R., Bottke, W. F., et al. 2023, AJ, 166, 55
Nesvorný, D., Vokrouhlický, D., Shelly, F., et al. 2024a, Icarus, 411, 1159222
Nesvorný, D., Vokrouhlický, D., Shelly, F., et al. 2024b, Icarus, 417, 116110
Park, R. S., Folkner, W. M., Williams, J. G., et al. 2021, AJ, 161, 105
Raab, H. 2012, Astrophysics Source Code Library, Astrometrica: Astrometric data reduction of CCD images. ascl:1203.012
Schirmer, M. 2013, ApJS, 209, 21
Schmithuesen, O., Erben, T., Trachternach, C., et al. 2007, Astron. Nachr., 328, 701
Scholl, H. & Froeschle, C. 1986, A&A, 170, 138
Schwartz, M. & Holvorcem, P. R. 2016, Minor Planet Electronic Circulars, 2016-T114.
Sidorenko, V. V. 2018, Cel. Mech. Dyn. Astron., 130, 4
Tremaine, S. 2023, MNRAS, 522, 937
Tudor, V., Vaduvescu, O., & Hudin, L. 2014, Minor Planet Electronic Circulars, 2014-L33
Vaduvescu, O., Birlan, M., Colas, F., et al. 2008, Planet. Space Sci., 56, 1913
Vaduvescu, O., Birlan, M., Tudorica, A., et al. 2011, Planet. Space Sci., 59, 1632
Vaduvescu, O., Hudin, L., Tudor, V., et al. 2015, MNRAS, 449, 1614
Vaduvescu, O., Hudin, L., Mocnik, T., et al. 2018, A&A, 609, A105
Vinogradova, T. A. 2017, MNRAS, 468, 4719
Vinogradova, T. A. 2024, Celest. Mech. Dyn. Astron., 136, 17
von Zeipel, H. 1910, Astron. Nachr., 183, 345
Zhou, J.-L. & Sun, Y.-S. 2003, ApJ, 598, 1290

Table A.1. Heliocentric Keplerian orbital elements of asteroid 622577 Miorita (2014 LU_{14}).

Parameter		Miorita
Semimajor axis, a (au)	=	1.28685458±0.00000002
Eccentricity, e	=	0.4496381±0.0000004
Inclination, i (°)	=	25.31145±0.00004
Longitude of the ascending node, Ω (°)	=	274.08069±0.00003
Argument of perihelion, ω (°)	=	219.48826±0.00005
Mean anomaly, M (°)	=	282.88704±0.00004
Perihelion, q (au)	=	0.7082358±0.0000004
Aphelion, Q (au)	=	1.86547339±0.00000003
MOID with the Earth (au)	=	0.197461
Absolute magnitude, H (mag)	=	19.71
Data-arc span (d)	=	3644
Number of observations	=	95

Notes. Values include the 1σ uncertainty. The orbit of Miorita (solution date, May 26, 2024, 05:47:28 PDT) is referred to epoch JD 2460800.5, which corresponds to 0:00 on 2025 May 5 TDB (Barycentric Dynamical Time, J2000.0 ecliptic and equinox). Source: JPL's SBDB.

Appendix A: Discovery and follow-up observations

Apollo-class NEA 622577 Miorita (2014 LU_{14}) was discovered serendipitously in observations of the proposal C136 (PI: O. Vaduvescu) aimed at recovering poorly studied NEAs by triggering max 1 h/night shots (sometimes including twilight time) using the 2.5 m-INT. Our program lasted five semesters, thus after two and a half years our collaboration recovered and made it possible to improve the orbital solutions of 280 faint NEAs (centered around $V \sim 22.8$ mag). In addition, we reported positions of about 3,500 known minor planets and another 1,500 unknown objects, producing the first nine EURONEAR serendipitous NEA discoveries (Vaduvescu et al. 2018).

As part of our C136 NEA recovery program and during the morning of June 1–2, 2014, we attempted the recovery of three known NEA, including the known target NEA 486001 (2012 MR_7), which was observed in the morning due to its relatively low Solar elongation (ϵ=117°). The discovery of Miorita was mainly due to chance, because it happened during the second recovery attempt of the known target, which was repeated due to a pointing error made one night prior.

Thanks to the possibility of triggering short INT service time slots during most nights when the Wide Field Camera (WFC) was available, we succesfully recovered Miorita on the second night and we could perform follow-up observations during five nights. For 18 days, no other major survey or individual observer was able to report it (MPS 518060, 518856) until it was confirmed from Cerro Tololo and Mount John (after the full moon), then by Pan-STARRS and Mauna Kea, which extended the data-arc to almost three months. Its orbital solution as of June 15, 2025, is shown in Table A.1.

A.1. Image reduction

During the entire recovery program, we promptly reduced the images (usually during the following morning) using the GUI version of the `THELI` software[9] (Schmithuesen et al. 2007; Schirmer 2013) which corrects for bias, flat, and field distortion, an issue that is very important for older telescopes and prime focus instruments such as the WFC. The actual observer and *THELI* reducer of the three fields observed during the discovery night was Vlad Tudor, an Isaac Newton Group of Telescopes (ING) student and INT support astronomer who promptly reduced all the fields.

For the actual moving object search and recovery of the NEA targets, a team of a few amateur astronomers used `Astrometrica`[10] (Raab 2012) to carefully scan all reduced images, visually blinking and measuring all moving sources, including the main target, plus any other known and unknown asteroids. The actual reducer of the three observed fields where Miorita was first found was Lucian Hudin, an amateur astronomer from Cluj-Napoca, Romania.

Finally, the NEA targets of the actual main program, plus the known and unknown detections in the observed fields were checked and promptly reported to the Minor Planet Center (MPC), usually during the next day, allowing the PI to eventually plan for the rapid recovery of any new NEA candidates, using the same INT program or asking other members of the EURONEAR network[11] with access to other telescopes.

A.2. NEA candidate EUHT171 = 622577 Miorita (2014 LU_{14})

Lucian Hudin identified 15 moving sources in the targeted field, including the main target NEA 486001 (recovered about 40" away from the official MPC ephemerides), other five known main belt asteroids (MBAs), and nine other unknown detections, which included Miorita. In order to perform quality control checks, during the entire program, we used the MPC `NEO Rating` tool[12] to check for possible NEO candidacy of all unknown detections. Miorita had the highest rating out of the 15 detections in this field (99%), then 35123 (74%, actually an MBA), then EUHT173 (71%).

As an additional quality control check, Vaduvescu et al. (2011) published a simple solar elongation–proper motion or ϵ–μ model assuming circular and coplanar orbits, which was later implemented online in our EURONEAR `NEA Checker` tool[13] aimed at assessing possible NEA candidates in any observed field. Figure A.1 presents the output for this field, from which Miorita and another unknown detection clearly stand up in comparison with the rest of the objects.

With a proper motion $\mu = 0.92''$/min, in the top panel of Fig. A.1, Miorita stands just above the border line (dotted magenta) which marks the separation between MBAs and NEA candidates in the ϵ–μ model. The main target (known NEA 486001) stands below the magenta line, and another similar detection (EUHT173) stands just below the border, being identified much later by the MPC as MBA 446534 (2014 MP_{14}) that was discovered in 2010 by the WISE survey (one month arc) and actually recovered by our program (MPS 521453),

On the middle and especially the bottom EURONEAR `NEA Checker` plot in Fig. A.1, Miorita clearly detaches as a NEA candidate, particularly due to the position angle, clearly different from those of all other known and unknown MBAs (including the known NEA target 486001). Actually, this direction of motion was clearly detected visually by the reducer who promptly informed the PI and reported the new NEO candidate EUHT171 (which eventually became Miorita) only two and half hours after the observations were completed.

[9] https://astro.uni-bonn.de/theli/

[10] http://www.astrometrica.at/

[11] http://www.euronear.org/network.php

[12] https://minorplanetcenter.net/iau/NEO/PossNEO.html

[13] http://www.euronear.org/tools/NEACheck.php

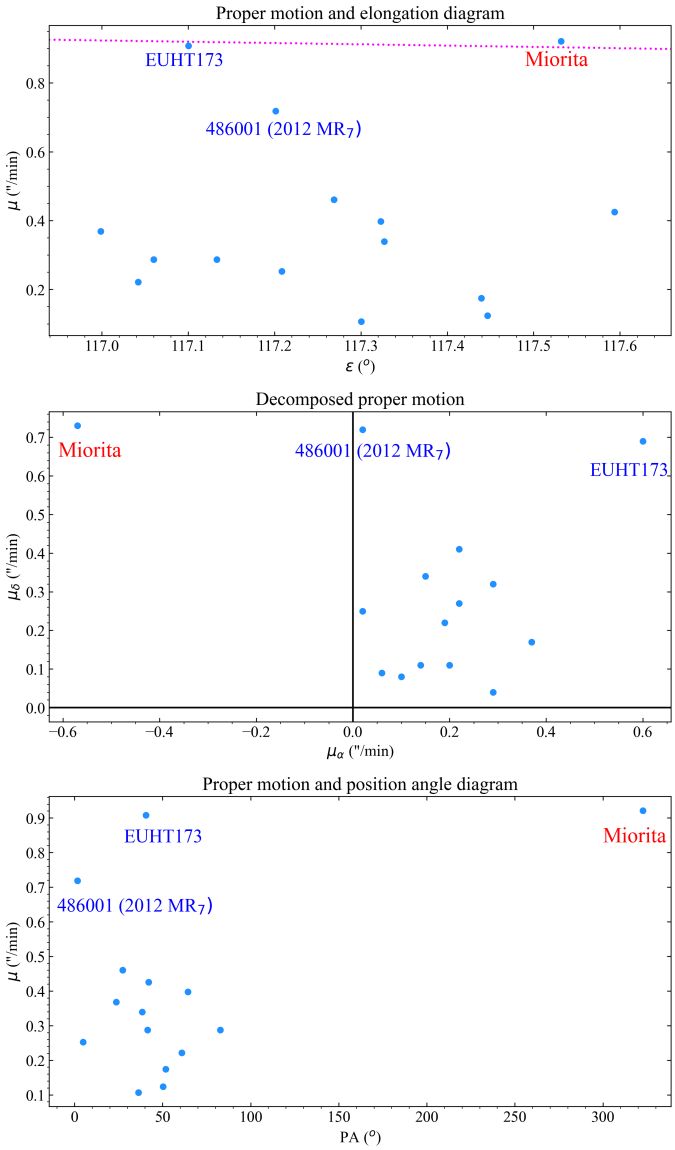

Fig. A.1. Observational details of the discovery of 622577 Miorita (2014 LU_{14}). *Top panel:* Results from the solar elongation–proper motion or ϵ–μ tool (in magenta). *Middle panel:* Proper motions in equatorial coordinates. *Bottom panel:* Proper motions as a function of the position angle.

Appendix B: Input data and uncertainties

Here, we include the barycentric Cartesian state vectors of 622577 Miorita (2014 LU_{14}) and other objects used in the calculations. These vectors and their uncertainties were used to perform the calculations discussed above. As an example, a new value of the X-component of the state vector was computed using $X_c = X + \sigma_X\, r$, where r is an univariate Gaussian random number, and X and σ_X are the mean value and its 1σ uncertainty in, e.g., Table B.1.

Appendix C: Miorita-like orbits

Figures C.1 and C.2 show the evolution over time of $\varpi - \varpi_5$ for 622577 Miorita (2014 LU_{14}) from the same simulations presented in the central and right panels of Fig. 1, respectively. The short-term evolution in Fig. C.1 shows an oscillation of $\varpi - \varpi_5$ that hints at an apsidal resonance with Jupiter for the control orbits, but the longer-term evolution in Fig. C.2 is more consistent with a near apsidal resonance with episodes of actual capture.

Figure C.3 shows the evolution of NEAs 387668 (2002 SZ), 2004 US_1, 299582 (2006 GQ_2), and 2018 AC_4, whose current orbits resemble that of Miorita. As Miorita, they are subjected to a von Zeipel-Lidov-Kozai secular resonance, but they are also in a near apsidal resonance, both controlled by Jupiter.

Table B.1. Barycentric Cartesian state vector of 622577 Miorita (2014 LU_{14}): Components and associated 1σ uncertainties.

Component		value$\pm1\sigma$ uncertainty
X (au)	=	$1.261525087989501\times10^{0}\pm7.81332354\times10^{-7}$
Y (au)	=	$1.415510074085832\times10^{-1}\pm1.65373719\times10^{-6}$
Z (au)	=	$6.025009389672883\times10^{-1}\pm8.41469560\times10^{-7}$
V_X (au/d)	=	$-6.778246475904528\times10^{-3}\pm1.24123060\times10^{-8}$
V_Y (au/d)	=	$1.165360296974367\times10^{-2}\pm3.75642625\times10^{-9}$
V_Z (au/d)	=	$-2.808860650274434\times10^{-3}\pm6.24561137\times10^{-9}$

Notes. Data are referred to epoch JD 2460800.5, which corresponds to 0:00 on 2025 May 5 TDB (J2000.0 ecliptic and equinox). Source: JPL's `Horizons`.

Table B.2. Barycentric Cartesian state vector of 504181 (2006 TC): Components and associated 1σ uncertainties.

Component		value$\pm1\sigma$ uncertainty
X (au)	=	$1.366245574867315\times10^{0}\pm6.59043937\times10^{-7}$
Y (au)	=	$1.502962644075712\times10^{0}\pm7.34785032\times10^{-7}$
Z (au)	=	$-7.019420919109259\times10^{-1}\pm7.14488621\times10^{-7}$
V_X (au/d)	=	$-8.212543579595001\times10^{-3}\pm4.84273509\times10^{-9}$
V_Y (au/d)	=	$-3.030690816816023\times10^{-3}\pm5.33875719\times10^{-9}$
V_Z (au/d)	=	$2.328011259580962\times10^{-3}\pm2.92860933\times10^{-9}$

Notes. Data are referred to epoch JD 2460800.5, which corresponds to 0:00 on 2025 May 5 TDB (J2000.0 ecliptic and equinox). Source: JPL's `Horizons`.

Table B.3. Barycentric Cartesian state vector of 482798 (2013 QK_{48}): Components and associated 1σ uncertainties.

Component		value$\pm1\sigma$ uncertainty
X (au)	=	$1.391336477097777\times10^{-1}\pm2.32350669\times10^{-6}$
Y (au)	=	$-5.133164792230683\times10^{-1}\pm1.34983145\times10^{-6}$
Z (au)	=	$1.057528256547908\times10^{-1}\pm2.10296029\times10^{-7}$
V_X (au/d)	=	$2.656004142457892\times10^{-2}\pm2.78143263\times10^{-8}$
V_Y (au/d)	=	$-1.428199888293871\times10^{-2}\pm8.35894569\times10^{-8}$
V_Z (au/d)	=	$-1.858328267787350\times10^{-3}\pm1.77818390\times10^{-8}$

Notes. Data are referred to epoch JD 2460800.5, which corresponds to 0:00 on 2025 May 5 TDB (J2000.0 ecliptic and equinox). Source: JPL's `Horizons`.

Appendix D: Long-term evolution of Miorita-like orbits

Figure D.1, left panels, shows the evolution into the future of the control orbit with state vectors separated -3σ from the nominal ones, this relevant clone appears in lime in the right panels of Fig. 1. It shows correlated long-period (~2 Myr) oscillations in the values of e and i, middle and bottom panels, respectively. These oscillations are linked to the apsidal resonance with Jupiter discussed in Sect. 4. Figure D.1 also shows the past and future evolution of the nominal orbits (see Table D.1) of

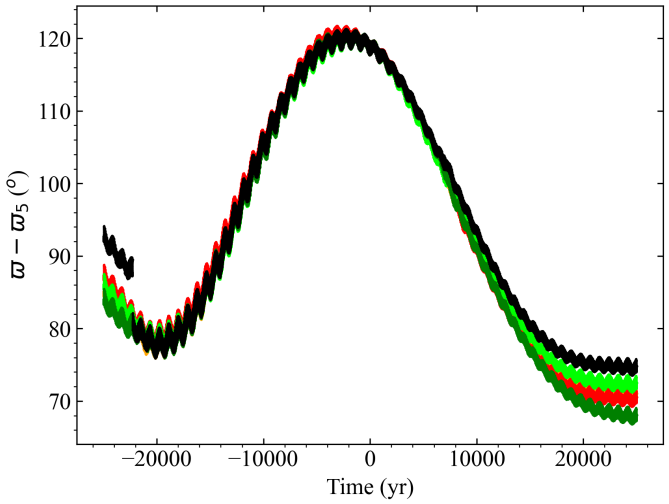

Fig. C.1. Time evolution of the apsidal longitude $\varpi - \varpi_5$ of 622577 Miorita (2014 LU_{14}). Results from the calculations displayed in the central panels of Fig. 1. Nominal orbit in black, those of control orbits with state vectors separated $\pm 3\sigma$ from the nominal ones in lime/green, and $\pm 9\sigma$ in orange/red. The source of the input data is JPL's `Horizons`.

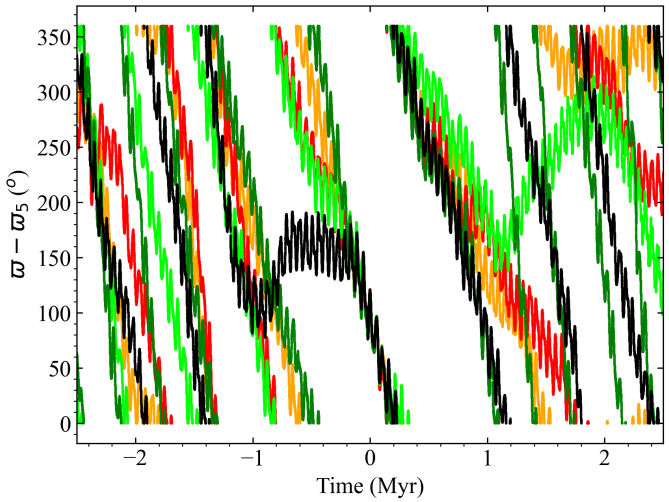

Fig. C.2. Time evolution of the apsidal longitude $\varpi - \varpi_5$ of 622577 Miorita (2014 LU_{14}). Results from the calculations displayed in the right panels of Fig. 1. Nominal orbit in black, those of control orbits with state vectors separated $\pm 3\sigma$ from the nominal ones in lime/green, and $\pm 9\sigma$ in orange/red. The source of the input data is JPL's `Horizons`.

504181 (2006 TC), central panels, and 482798 (2013 QK_{48}), right panels, the input state vectors appear in Tables B.2 and B.3. Masiero et al. (2024) have suggested that 504181 might be the largest fragment of the asteroid breakup that created the Phaethon–Geminid complex. Apollo-class NEA 482798 is a PHA that experiences relatively close encounters with Mars, Venus and Mercury. In Fig. D.1, the nominal orbit of 482798 goes into the Sun both integrating forward and backwards.

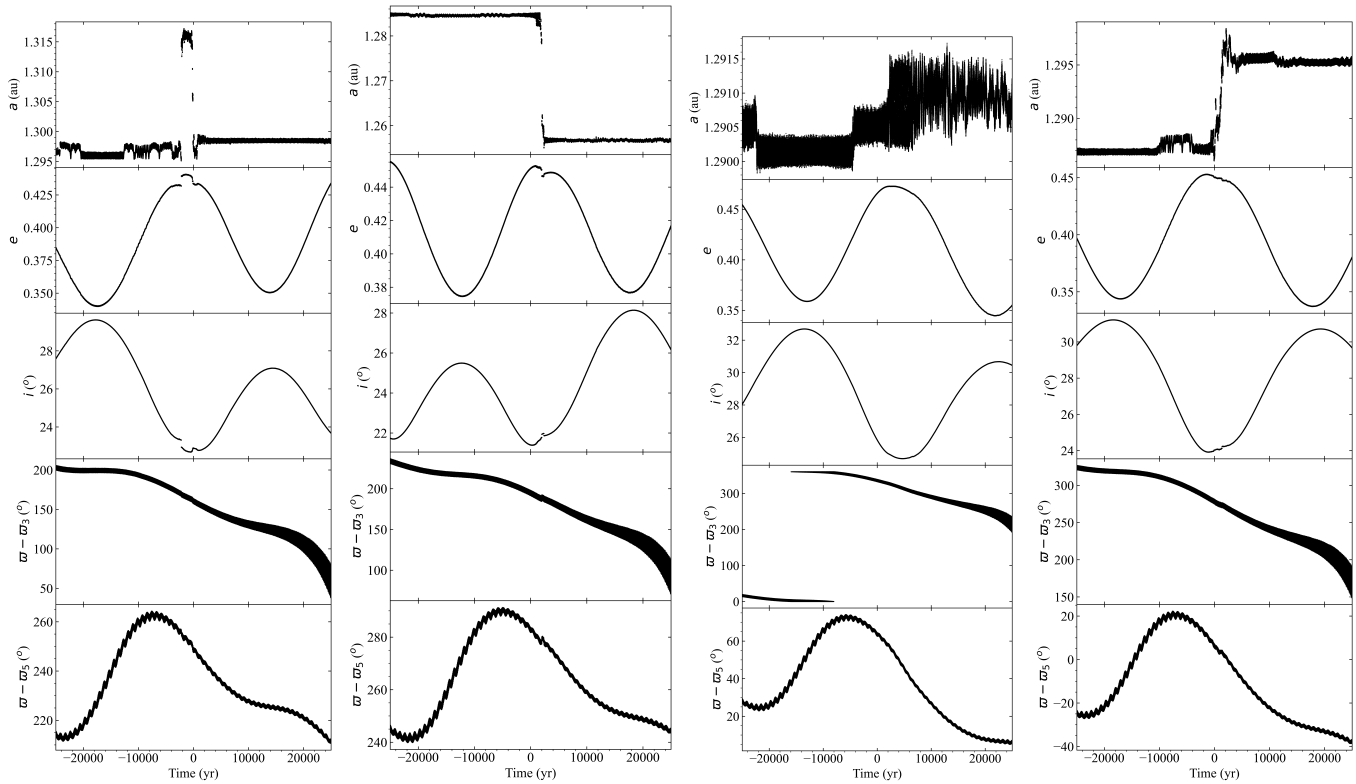

Fig. C.3. Orbital evolution of NEAs 387668 (2002 SZ), 2004 US_1, 299582 (2006 GQ_2), and 2018 AC_4. *Left panels:* Past and future evolution of the nominal orbit of 387668. *Second to left panels:* Past and future evolution of the nominal orbit of 2004 US_1. *Second to right panels:* Past and future evolution of the nominal orbit of 299582. *Right panels:* Past and future evolution of the nominal orbit of 2018 AC_4. Time evolution of the value of the semimajor axis, a (top panels), eccentricity, e (second to top), inclination, i (middle), the apsidal longitude relative to Earth, $\varpi - \varpi_3$ (second to bottom), and the apsidal longitude relative to Jupiter, $\varpi - \varpi_5$ (bottom). The origin of time is the epoch 2460800.5 JD Barycentric Dynamical Time (2025-May-05.0 00:00:00.0 TDB) and the output cadence is 36.525 d. The source of the input data is JPL's `Horizons`.

Table D.1. Heliocentric Keplerian orbital elements of asteroids 504181 (2006 TC) and 482798 (2013 QK_{48}).

Parameter		504181	482798
Semimajor axis, a (au)	=	1.53827035±0.00000002	1.58573770±0.00000002
Eccentricity, e	=	0.91204242±0.00000011	0.82973801±0.00000007
Inclination, i (°)	=	19.54779±0.00002	18.967424±0.000012
Longitude of the ascending node, Ω (°)	=	151.76208±0.00011	141.39855±0.00002
Argument of perihelion, ω (°)	=	61.51161±0.00010	47.18181±0.00002
Mean anomaly, M (°)	=	290.80622±0.00006	8.47648±0.00005
Perihelion, q (au)	=	0.1353025±0.0000002	0.26999085±0.00000011
Aphelion, Q (au)	=	2.94123816±0.00000004	2.90148454±0.00000004
MOID with the Earth (au)	=	0.144222	0.026112
Absolute magnitude, H (mag)	=	18.81	18.35
Data-arc span (d)	=	4792	8520
Number of observations	=	59	149

Notes. Values include the 1σ uncertainty. The orbits of 504181 (solution date, March 1, 2023, 06:49:57 PST) and 482798 (solution date, December 22, 2024, 05:28:42 PST) are referred to epoch JD 2460800.5, which corresponds to 0:00 on 2025 May 5 TDB (Barycentric Dynamical Time, J2000.0 ecliptic and equinox). Source: JPL's SBDB.

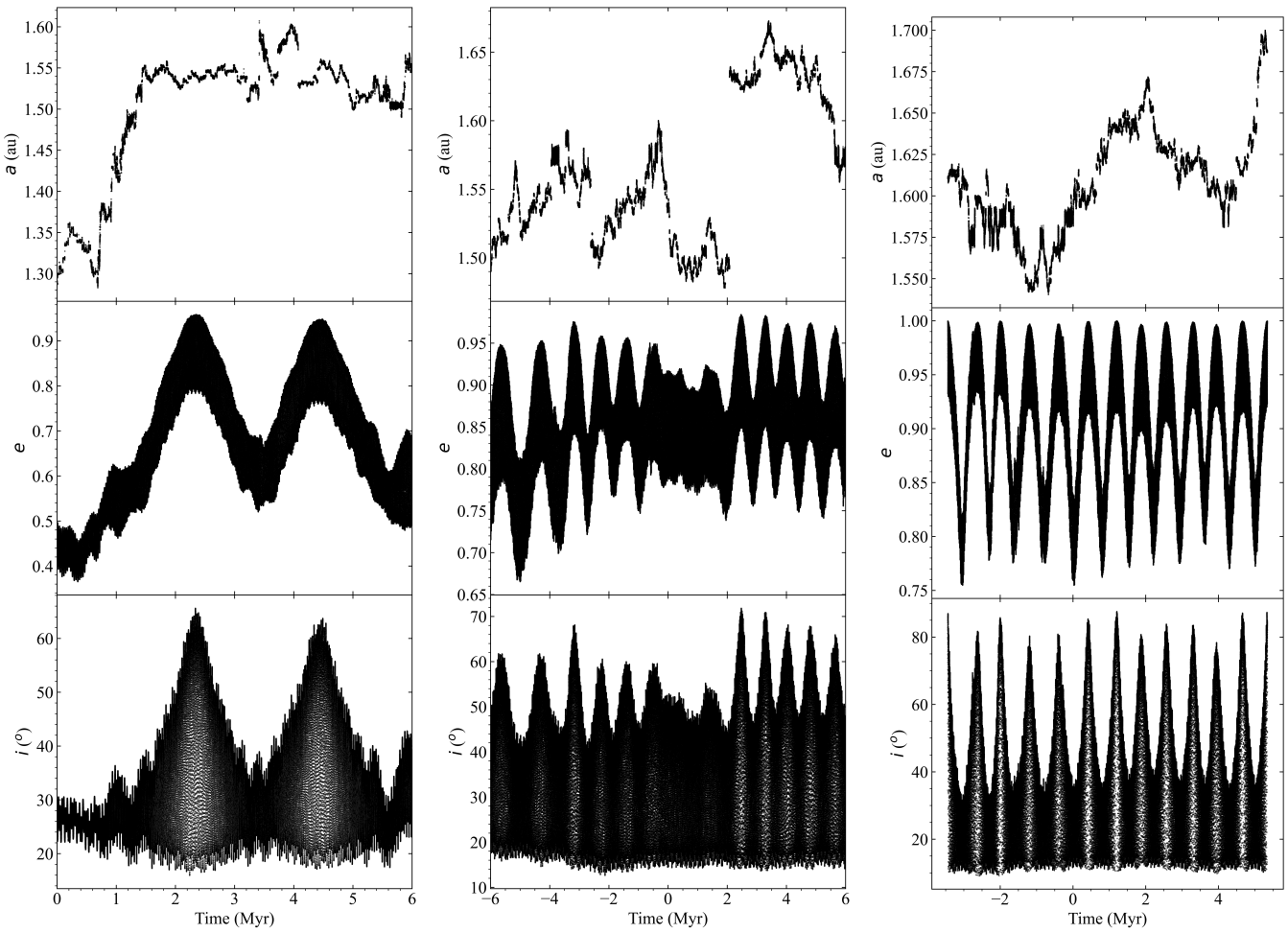

Fig. D.1. Orbital evolution of a representative control orbit of 622577 Miorita (2014 LU_{14}) and NEAs 504181 (2006 TC), and 482798 (2013 QK_{48}). *Left panels:* Future evolution of the control orbit with state vectors separated -3σ from the nominal ones, this relevant clone appears in lime in the right panels of Fig. 1. *Central panels:* Past and future evolution of the nominal orbit of 504181. *Right panels:* Past and future evolution of the nominal orbit of 482798. Time evolution of the value of the semimajor axis, a (top panels), eccentricity, e (middle), inclination, i (bottom). The origin of time is the epoch 2460800.5 JD Barycentric Dynamical Time (2025-May-05.0 00:00:00.0 TDB) and the output cadence is 36.525 d for the left and central panels, and 25 yr for the right panels. The source of the input data is JPL's `Horizons`.